Monte Carlo Estimation of Local Initial Error Growth

C. E. Leith

National Center for Atmospheric Research*
Boulder, Colorado 80307, U.S.A

October 1979

*The National Center for Atmospheric Research is sponsored by the National Science Foundation.

Abstract

Many predictability studies have provided global estimates of the mean error growth rate arising from the inherent instability of atmospheric flows. It is, however, of practical value and theoretical interest to determine the predictability of local synoptic situations. Monte Carlo experiments have been carried out with a spectral barotropic model in which randomly imposed perturbations induce perturbation tendency responses in the vorticity field. Maps of local root mean square response show preferred areas of error sensitivity in regions of maximum wind speed, as expected from error advection effects. Sampling fluctuations in the experiments, however, obscure the correlation of vorticity perturbation and response which might serve as a more precise measure of local stability and predictability.

Introduction

Studies of the predictability of the large-scale motions in the atmosphere have been concerned primarily with global estimates of the theoretically expected growth during predictions of the initial observation and analysis errors. This growth is recognized to be an inherent property of the nonlinear dynamics of the atmosphere which would occur even with a perfect prediction model. Model imperfections provide, of course, an additional important source of error growth.

It is the purpose of this paper to examine the problem of local predictability, that is, the determination of the error growth for different regions of a given synoptic state. This is one of the main objectives of stochastic dynamic prediction methods in which the evolution of an ensemble of forecasts is considered. There is no need to elaborate on the practical value of being able to attach a level of confidence to a particular local forecast. There is also, however, considerable theoretical interest in attempting to measure the relative stability and predictability of local flow structures such as occur, for example, in atmospheric blocking situations.

Stochastic dynamic methods have been used to examine error growth over several days, but this paper will concentrate on the initial growth that can be related to the existing synoptic state. This problem is closely related to the problem of determining the stability of small perturbations to a specified flow field. In general the associated stability matrix is of a dimension too great for feasible algebraic analysis, and so Monte Carlo approximations are developed.

A spectral barotropic model is used for these experiments in order to avoid the additional difficulties that arise from the influence of unbalanced gravitational modes on initial tendencies. It is found that the Monte Carlo method is not particularly effective in finding unstable modes but does show that local error sensitivity is associated with large wind speed. This result is not surprising and is consistent with error results for 2-day forecasts made with a similar model and verified against the real atmosphere.

Stability matrix

For an abstract model dynamical equation

$$\dot{\underset{\sim}{x}} = \underset{\sim}{q}(\underset{\sim}{x})$$

the dynamical state column vector $\underset{\sim}{x}$ evolves in accordance with the generally nonlinear dynamics given by the vector function $\underset{\sim}{q}(\underset{\sim}{x})$. As a model, the dynamical system has a large but finite number of degrees of freedom, D, which is the dimensionality of the vectors $\underset{\sim}{x}$ and $\underset{\sim}{q}$.

An infinitesimal perturbation $\delta\underset{\sim}{x}$ in the state vector produces a perturbation $\delta\dot{\underset{\sim}{x}}$ in the tendency of $\underset{\sim}{x}$ given by

$$\delta\dot{\underset{\sim}{x}} = \underset{\sim}{P}\,\delta\underset{\sim}{x} \quad ,$$

where the matrix elements of $\underset{\sim}{P}$ are the partial derivatives of the components of $\underset{\sim}{q}$ with respect to those of $\underset{\sim}{x}$, symbolically

$$\underset{\sim}{P} = \left\{ \frac{\partial \underset{\sim}{q}}{\partial \underset{\sim}{x}} \right\} \quad .$$

We shall call $\underset{\sim}{P}$ the stability matrix which, for the general nonlinear dynamics of interest here, is a function of the basic unperturbed state vector $\underset{\sim}{x}$.

In principle, all linear stability questions can be answered in terms of algebraic analyses of the matrix $\underset{\sim}{P}$. For example, any eigenvector of $\underset{\sim}{P}$ for which the corresponding eigenvalue has a positive real part represents an unstable perturbation mode.

In practice there are difficulties with the analysis of $\underset{\sim}{P}$. For systems with the number of degrees of freedom D greater than of order 100, the necessary manipulations of DxD matrices become computationally

cumbersome. The usual methods of functional analysis are not applicable since $\underset{\sim}{P}$ is not normal (i.e., does not commute with its adjoint). And, finally, the analysis of $\underset{\sim}{P}$ provides more global than local information.

The usual predictability problem is to determine the expected growth of average error variance. If averages are taken over all the degrees of freedom of the system and over an ensemble of perturbations, then the average error variance is given by

$$E = \varepsilon^2 = (1/D)\ \mathrm{Tr} \langle \underset{\sim}{\delta x}\ \underset{\sim}{\delta x}^* \rangle \quad ,$$

where an asterisk indicates the complex conjugate transpose. In this case $\underset{\sim}{\delta x}^*$ is the row vector transpose of the real perturbation column vector $\underset{\sim}{\delta x}$. The trace symbol Tr indicates summation over the diagonal elements of the covariance matrix $\langle \underset{\sim}{\delta x}\ \underset{\sim}{\delta x}^* \rangle$, so that ε^2 is the mean square of the components of $\underset{\sim}{\delta x}$.

We shall assume that at time t = 0 errors are imposed with variance uniform in the components of $\underset{\sim}{\delta x}$ thus that

$$\langle \underset{\sim}{\delta x}\ \underset{\sim}{\delta x}^* \rangle = \varepsilon^2\ \underset{\sim}{I} \quad ,$$

where $\underset{\sim}{I}$ is the identity matrix.

Consider now the initial behavior of $E = \varepsilon^2$ starting from t = 0 in an expansion through terms quadratic in t.

$$E(t) = E(o) + t\,\dot{E}(o) + \frac{1}{2}\,t^2\,\ddot{E}(o) \quad .$$

The first time derivative $\dot{E}$ is given simply by

$$\dot{E} = (1/D)\ \mathrm{Tr}\ [\langle \dot{\delta x}\ \delta x^{*}\rangle + \langle \delta x\ \dot{\delta x}^{*}\rangle]$$

$$= (1/D)\ \mathrm{Tr}\ [P\ \langle \delta x\ \delta x^{*}\rangle + \langle \delta x\ \delta x^{*}\rangle\ P^{*}]$$

$$= (1/D)\ \mathrm{Tr}\ [P + P^{*}]\ E \quad .$$

The second time derivative, however, depends in part on an evaluation of

$$\ddot{\delta x} = \dot{P}\ \delta x + P\ \dot{\delta x} \quad .$$

We introduce a new matrix

$$Q(x) = \frac{\partial P(x)}{\partial x}\ q(x)$$

$$= \frac{\partial P(x)}{\partial x}\ \dot{x} = \dot{P}$$

in terms of which we may write

$$\ddot{\delta x} = (Q + P^{2})\ \delta x \quad .$$

The second time derivative $\ddot{E}$ is given then by

$$\ddot{E} = (1/D)\ \mathrm{Tr}\ [\langle \delta x\ \ddot{\delta x}^{*}\rangle + 2\ \langle \dot{\delta x}\ \dot{\delta x}^{*}\rangle + \langle \ddot{\delta x}\ \delta x^{*}\rangle]$$

$$= (1/D)\ \mathrm{Tr}\ [(Q + Q^{*}) + (P + P^{*})^{2}]\ E$$

and the initial behavior of $E = \varepsilon^{2}$ is given by

$$E(t) = [1 + t\ (1/D)\ \mathrm{Tr}\ (P + P^{*}) + \tfrac{1}{2}\ t^{2}\ (1/D)\ \mathrm{Tr}\{(Q + Q^{*}) + (P + P^{*})^{2}\}]\varepsilon^{2} \quad .$$

We shall have occasion to refer later to a truncated version of this expression

$$\tilde{E}(t) = [1 + t\ (1/D)\ \mathrm{Tr}\ (P + P^{*}) + t^{2}\ (1/D)\ \mathrm{Tr}\ (P\ P^{*})]\ \varepsilon^{2} \quad .$$

Spectral barotropic model

The dynamical model used for the experiments described in this paper is a spectral barotropic model of strictly nondivergent motion. A spectral transform algorithm is used which is the appropriate simplification of that used by Bourke (1972) for a shallow water primitive equation model. Triangular truncation $0 \leq m < n \leq N = 18$ provides $D = 170$ essential degrees of freedom. The basic state vector x is taken to be a representation of the 500 mb vorticity field for which values are obtained by a linear balance relation applied to a spectral representation of the 500 mb geopotential field as analyzed by the U.S. National Meteorological Center. Only antisymmetric modes with n-m odd are kept to describe the vorticity field in the northern hemisphere. The model is thus similar to that used for earlier forecasting experiments (Leith, 1974), but no correction is introduced for climatological mean tendency, nor are free surface effects included.

The dynamics equation, therefore, becomes simply

$$\frac{\partial \xi}{\partial t} + J(\psi, f + \xi) = 0 \quad ,$$

with the stream field ψ related to the vorticity field ξ by the Poisson equation $\nabla^2 \psi = \xi$. We use an alias-free evaluation of the Jacobian $J(\psi, f + \xi)$ by the spectral transform method. The domain is the northern hemisphere with a frictionless wall at the equator.

In terms of the abstract formulation of the dynamics we may write then

$$\dot{\underset{\sim}{\xi}} = \underset{\sim}{q}(\underset{\sim}{\xi}) \quad .$$

Statistical analysis

In this paper we completely avoid the explicit evaluation of $\underset{\sim}{P}$ which might be carried out by evaluation of $\dot{\underset{\sim}{\xi}} = \underset{\sim}{q}(\underset{\sim}{\xi})$ once for $\underset{\sim}{\xi}$ unperturbed and D times for $\underset{\sim}{\xi}$ perturbed separately in each one of its D components. Instead, we wish to evaluate quantities of interest by Monte Carlo estimation of their statistical properties.

The matrix $\underset{\sim}{P}$, for example, is related to the covariance of $\delta\dot{\underset{\sim}{\xi}}$ and $\delta\underset{\sim}{\xi}$ since

$$<\delta\dot{\underset{\sim}{\xi}}\ \delta\underset{\sim}{\xi}^{*}> \ = \ \underset{\sim}{P}\ <\delta\underset{\sim}{\xi}\ \delta\underset{\sim}{\xi}^{*}> \ = \ \varepsilon^{2}\underset{\sim}{P} \ .$$

A Monte Carlo estimation of $<\delta\dot{\underset{\sim}{\xi}}\ \delta\underset{\sim}{\xi}^{*}>$ with a finite sample of size M involves M equations of $\delta\dot{\underset{\sim}{\xi}}$ and provides an estimate of $\underset{\sim}{P}$ which is, of course, contaminated by sampling fluctuations that decrease as M increases.

Although the usual global analysis of error growth averages over all degrees of freedom, we are in this case interested in the local error growth. Thus, we use a configuration space representation of matrices such as $<\delta\dot{\underset{\sim}{\xi}}\ \delta\underset{\sim}{\xi}^{*}>$ and consider only the diagonal elements which we display as maps. The matrix elements are real and the diagonal elements are unchanged by the adjoint operation. The global average operation (1/D) Tr becomes in this case a spatial average over the hemispherical domain.

Experimental results

The basic vorticity and associated stream field used in this study are mapped in Fig. 1. They are based on the NMC Northern Hemisphere analysis of geopotential height for 12Z, 6 December 1967.

For this basic state $\underset{\sim}{\xi}_o$ a calculation is made of $\underset{\sim}{\xi}_o = \underset{\sim}{q}(\underset{\sim}{\xi}_o)$ which serves as a reference. An ensemble of M perturbed states is then generated by addition of random Gaussian perturbations $\delta\xi_i$ to each component ξ_i of $\underset{\sim}{\xi}$ in its surface harmonic representation. The perturbations $\delta\xi_i$ are generated as independent random numbers from a Gaussian distribution with a standard deviation which is about 1% of typical vorticity components of the basic state.

In Fig. 2 there is shown a map of a typical vorticity perturbation field $\delta\underset{\sim}{\xi}$. These random fields are uncorrelated on the spatial scales resolved by the truncation that was imposed.

For each perturbation a nonlinear calculation is made to determine a response

$$\delta\dot{\underset{\sim}{\xi}} = \underset{\sim}{q}(\underset{\sim}{\xi}_o + \delta\underset{\sim}{\xi}) - \underset{\sim}{q}(\underset{\sim}{\xi}_o) \quad .$$

For the perturbation $\delta\underset{\sim}{\xi}$ displayed in Fig. 2, the response $\delta\dot{\underset{\sim}{\xi}}$ is mapped in Fig. 3.

The maps shown in Figs. 2 and 3 are based on the transformation of $\delta\underset{\sim}{\xi}$ and $\delta\dot{\underset{\sim}{\xi}}$ to a latitude-longitude grid with 5° resolution.

The perturbation calculation is repeated for an ensemble of M independent cases, and statistics are accumulated at gridpoints for estimation of

$$\langle(\delta\xi)^2\rangle = \text{diag}\ \varepsilon^2\ \underset{\sim}{I}$$

$$\langle(\delta\dot{\xi})(\delta\xi)\rangle = \text{diag}\ \varepsilon^2\underset{\sim}{P}$$

and

$$<(\delta\dot{\xi})^2> \;=\; \text{diag}\; \varepsilon^2 \underset{\sim}{P}\, \underset{\sim}{P}^*$$

where the operator diag selects the diagonal elements of the matrix for spatial mapping. The first of these statistics serves as a test of the adequacy of the sampling procedure since in the limit as $M \to \infty$ it should approach a constant independent of latitude and longitude. Fig. 4 shows the relative maxima and minima in a map of the square root of this first statistic, superimposed on a map of the basic stream field, for a sample of M = 100 perturbations. These have a distribution about a constant value which indicates the relative sampling fluctuation expected for such a sample.

By contrast to this root mean square perturbation $<(\delta\xi)^2>^{1/2}$ shown in Fig. 4 the root mean square response $<(\delta\dot{\xi})^2>^{1/2}$ shown in Fig. 5 differs significantly from a constant value. This measure of response which enters into the truncated quadratic error growth term shows definite maxima which appear to be situated in regions of maximum wind speed as shown by the superimposed stream field contours.

The covariance estimate of $<(\delta\dot{\xi})(\delta\xi)>$ is not mapped directly, but rather the sample correlation field estimating

$$r \;=\; \frac{<(\delta\dot{\xi})(\delta\xi)>}{<(\delta\dot{\xi})^2>^{1/2}\, <(\delta\xi)^2>^{1/2}} \quad ,$$

which is shown in percent in Fig. 6. This field is quite irregular and probably nowhere signficantly nonzero since for a sample of M = 100 and r = 0, variations in estimates of r of order ±10% would be expected from sampling fluctuations. It appears then that the individual diagonal elements of $\underset{\sim}{P}$ or of $1/2(\underset{\sim}{P} + \underset{\sim}{P}^*)$ are too small to be determined in this way.

The significant maxima of response shown in Fig. 5 suggest that the advection of error is a relatively important source of error growth. The same qualitative result can be inferred from error growth in real 48-hour forecasts with a similar model (Leith, 1974). An example is shown in Fig. 7. The forecast shown in Fig. 7 required 48 evaluations of the nonlinear term $\underset{\sim}{q}(\underset{\sim}{\xi})$, whereas the results shown in Fig. 5 required 101 evaluations.

Conclusions

From these experiments we may conclude that for the model used here the Monte Carlo estimation procedure was marginally able to identify error sensitive regions with an investment in computing comparable to that of a 2-day forecast.

Error sensitivity is related to the operator $\underset{\sim}{P}\underset{\sim}{P}^*$ whose positive real eigenvalues measure the squared magnitude of response of any kind. The real eigenvalues of $\underset{\sim}{P} + \underset{\sim}{P}^*$ are more relevant to stability and significant values of these were not identified by the Monte Carlo procedure.

These results are compatible with the suggestion that the ratio of the real and imaginary parts of the eigenvalues of $\underset{\sim}{P}$ is small. It is worth noting that for a basic state at rest the eigenvalues of $\underset{\sim}{P}$ are purely imaginary.

Further studies are needed to test the ability of Monte Carlo methods to estimate higher derivative covariances such as $\langle \delta\dot{\underset{\sim}{\xi}} \, \delta\underset{\sim}{\xi}^* \rangle$ accurately enough to determine the complete quadratic initial dependence of error growth on time.

References

Bourke, W., 1972: An efficient, one-level, primitive equation spectral model. Mon. Wea. Rev., 100, 683-689.

Leith, C. E., 1974: Spectral statistical-dynamical forecast experiments. Int. Symp. on Spectral Methods in Numerical Weather Prediction. Copenhagen, August 1974. GARP WGNE Report No. 7.

Figure captions

Fig. 1: Map of 500 mb absolute vorticity (solid) and stream field (dashed) for 12Z, 6 December 1967.

Fig. 2: Typical vorticity perturbation field.

Fig. 3: Vorticity tendency perturbation induced by the perturbation shown in Fig. 2.

Fig. 4: Root mean square vorticity perturbation.

Fig. 5: Root mean square vorticity tendency response.

Fig. 6: Correlation (in percent) of perturbation and response.

Fig. 7: Real 48-hour forecast error for forecast starting 00Z, 7 December 1967.

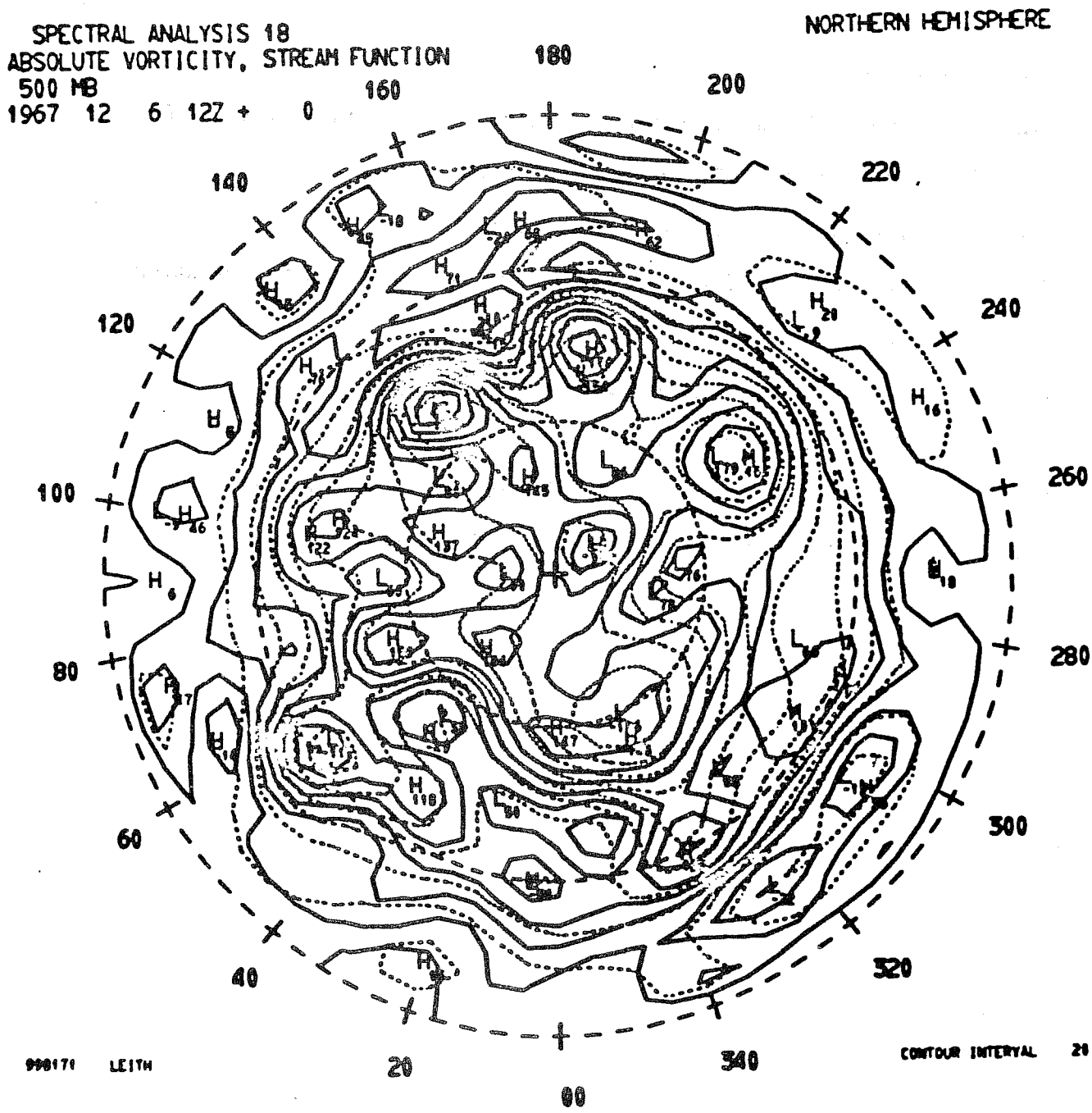

Fig. 1: Map of 500 mb absolute vorticity (solid) and stream field (dashed) for 12Z, 6 December 1967.

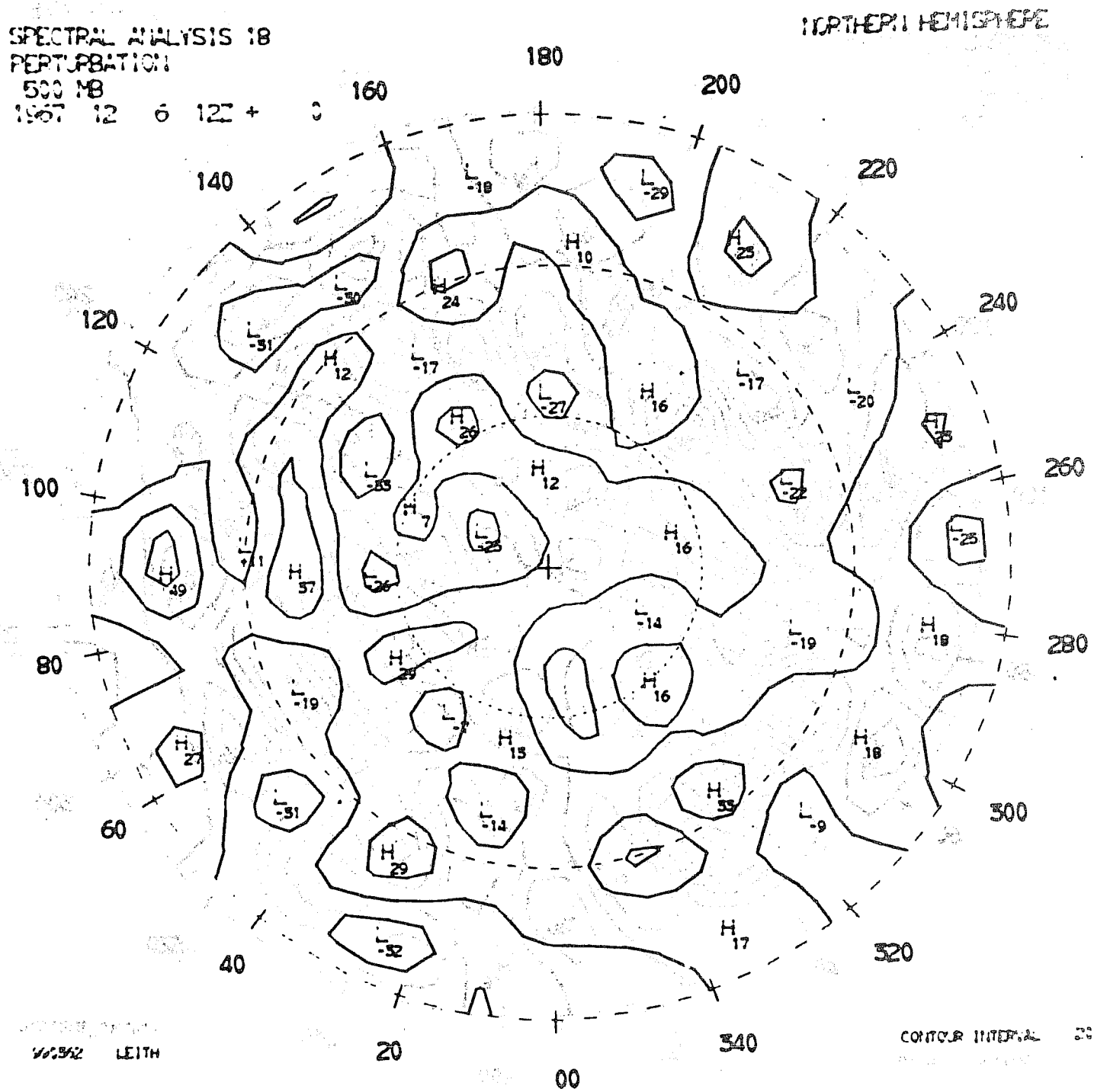

Fig. 2: Typical vorticity perturbation field.

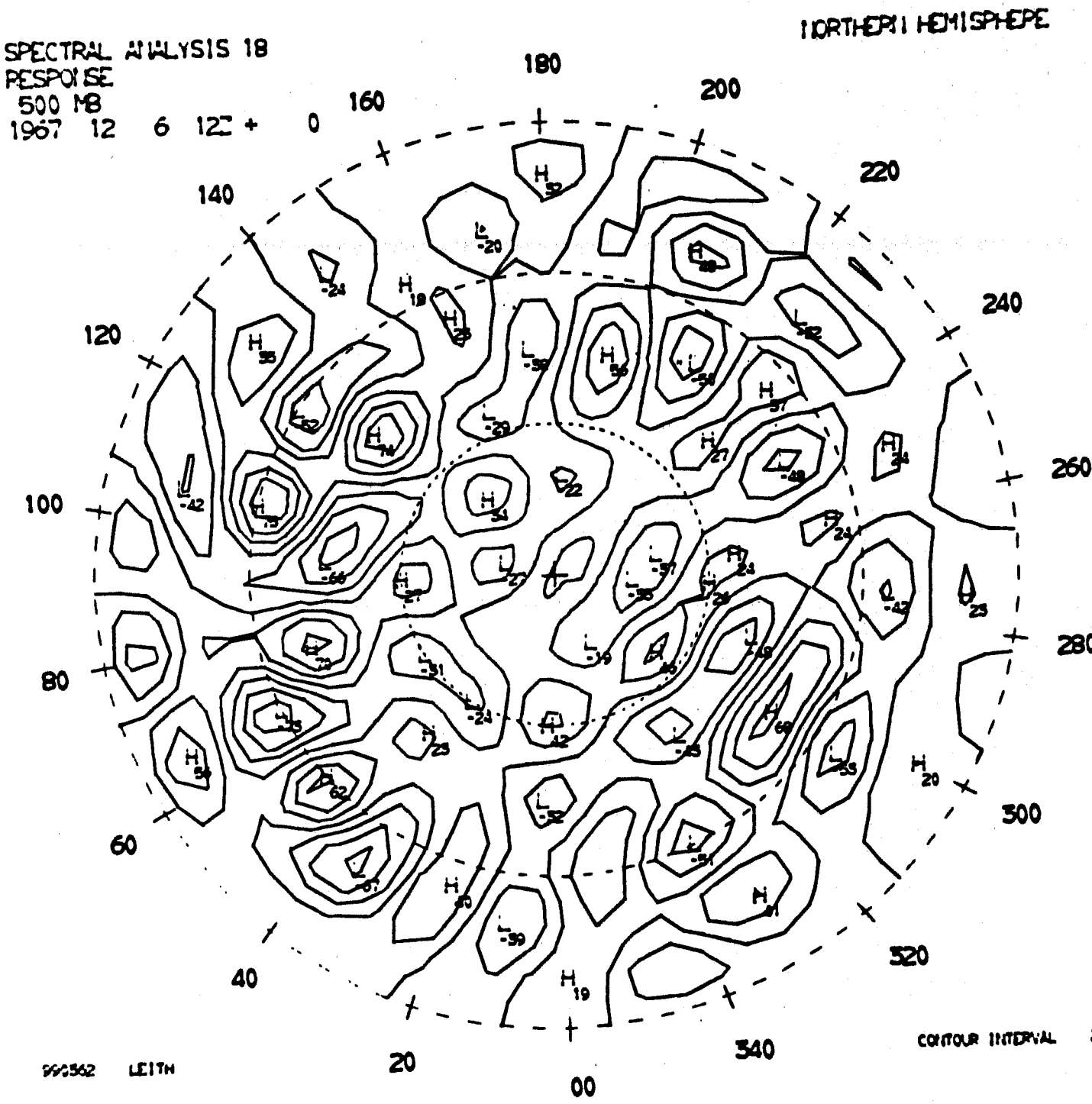

Fig. 3: Vorticity tendency perturbation induced by the perturbation shown in Fig. 2.

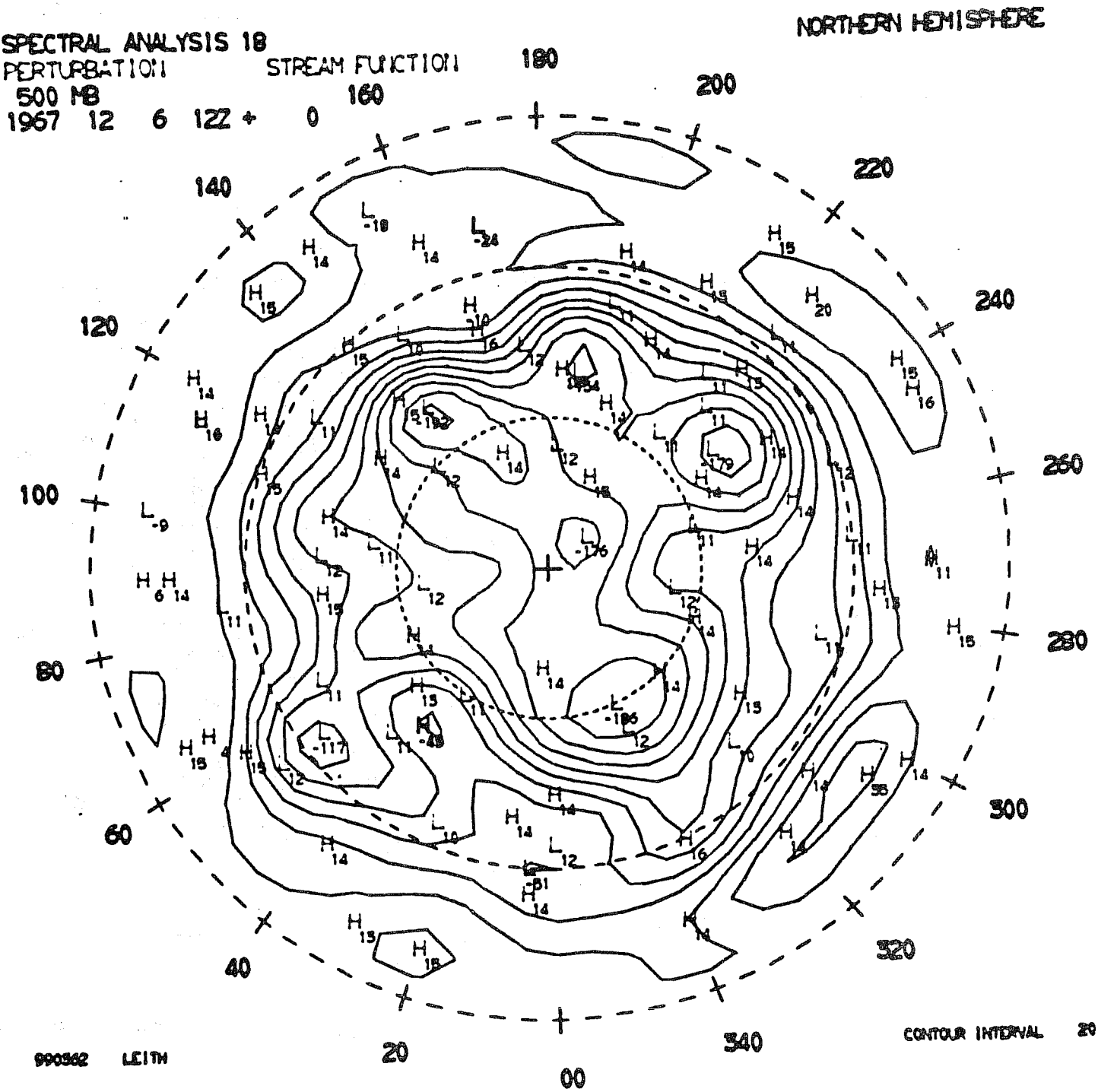

Fig. 4: Root mean square vorticity perturbation.

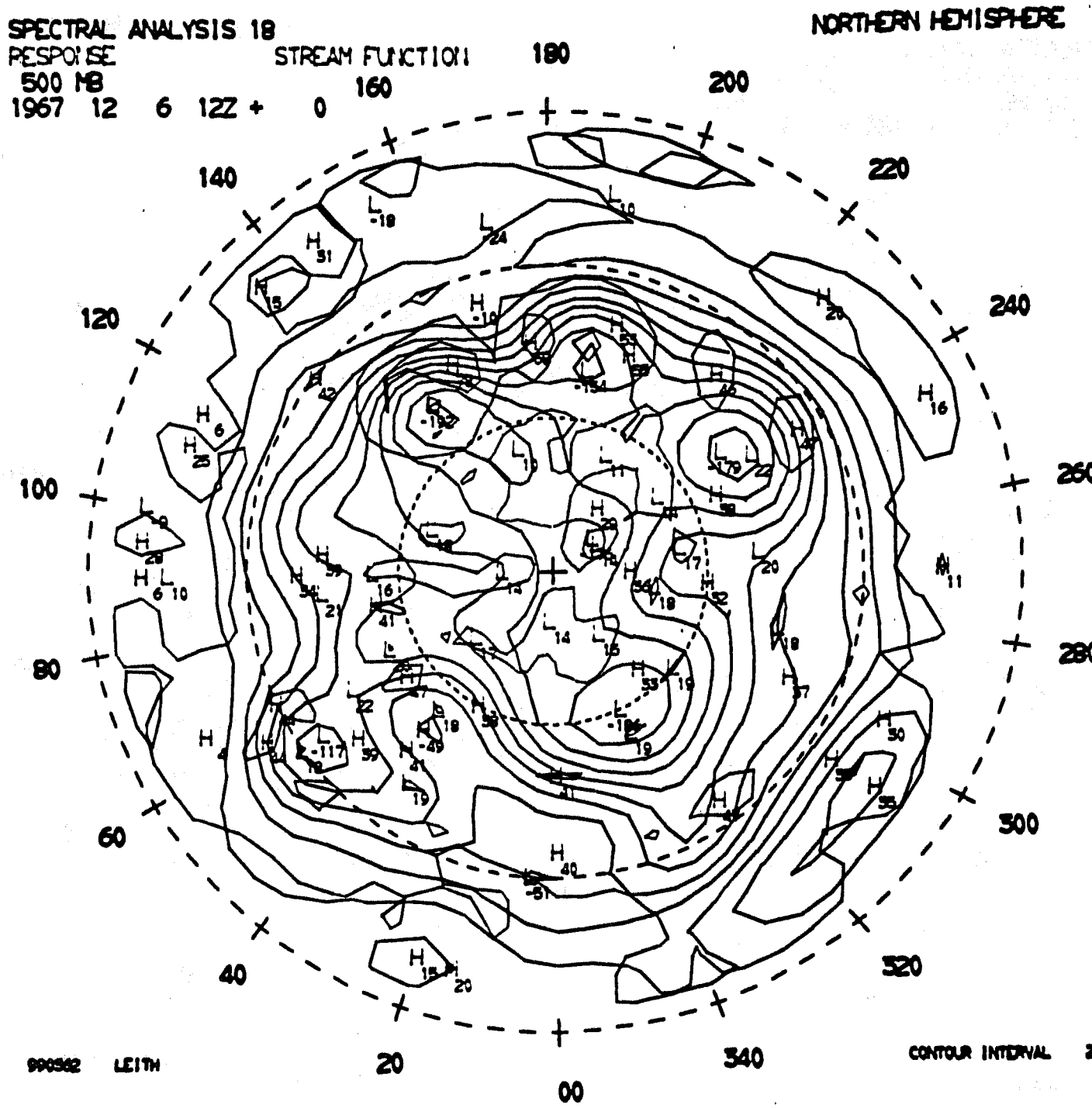

Fig. 5: Root mean square vorticity tendency response.

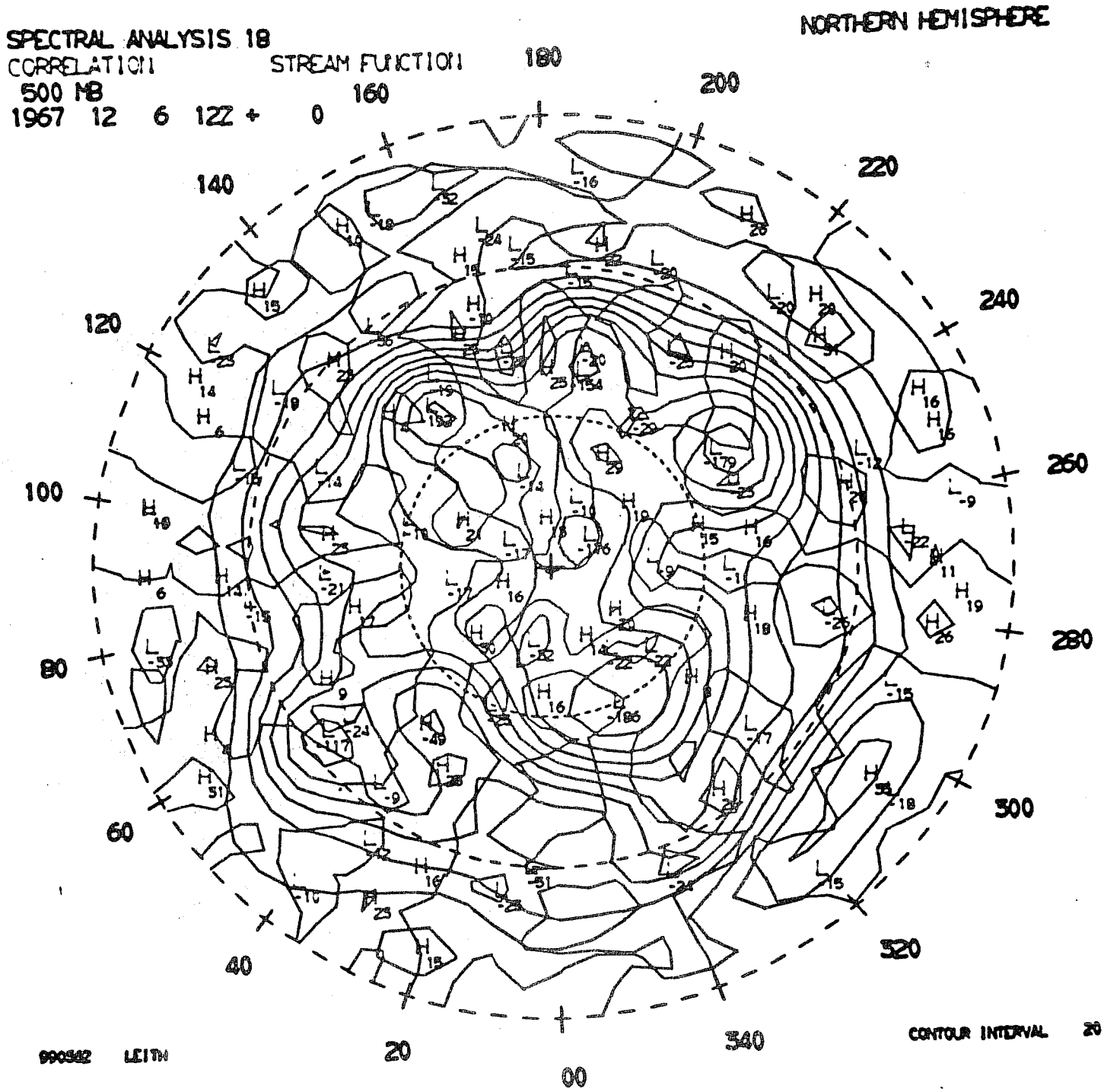

Fig. 6: Correlation (in percent) of perturbation and response.

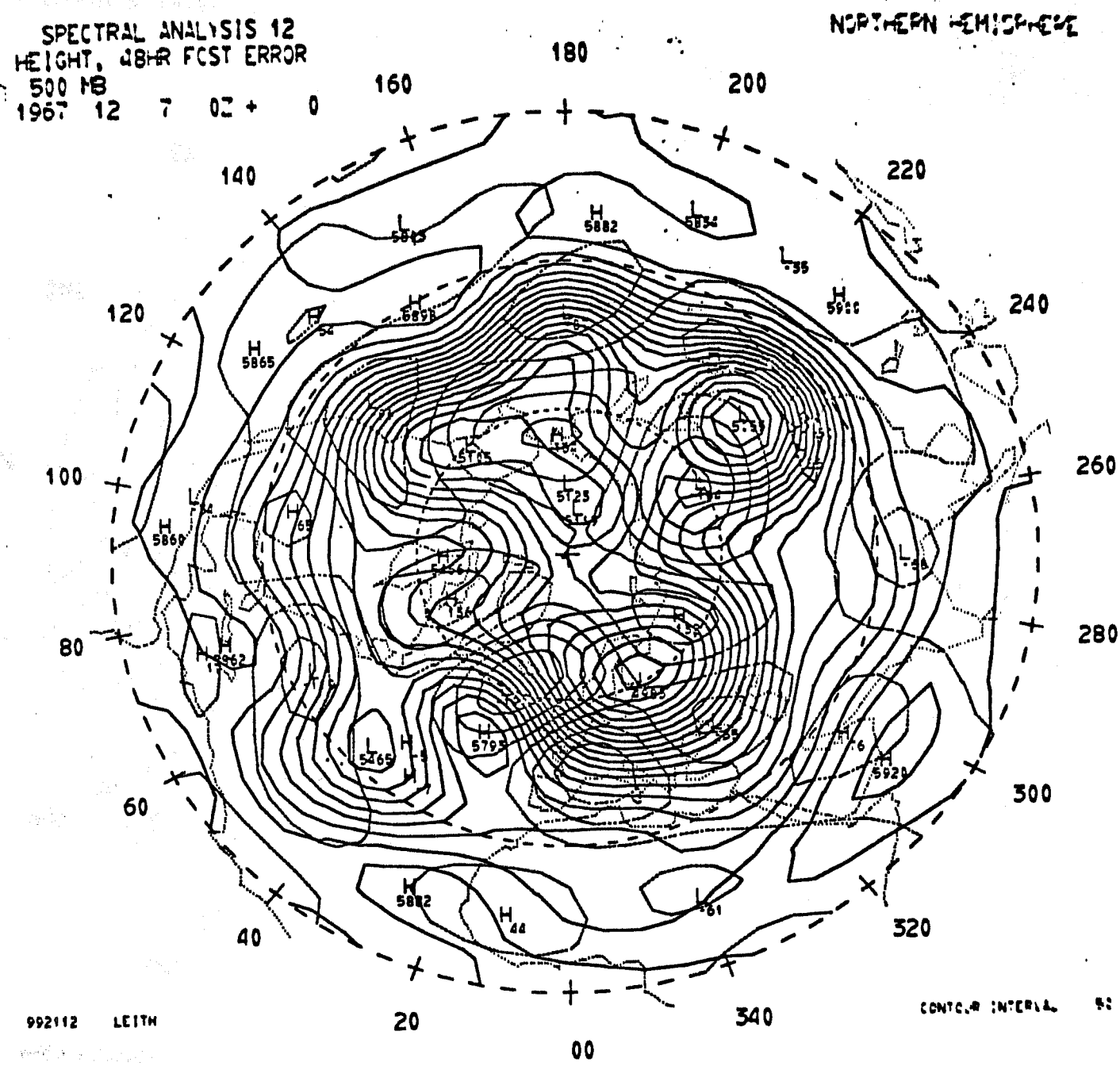

Fig. 7: Real 48-hour forecast error for forecast starting 00Z, 7 December 1967.